SVM Classification Study of Code–modulated Visual Evoked Potentials

Daiki Aminaka*, Shoji Makino*, and Tomasz M. Rutkowski*,†,▽
*Department of Computer Science and Life Science Center of TARA
University of Tsukuba
Tsukuba, Ibaraki, Japan
†RIKEN Brain Science Institute
Wako-shi, Saitama, Japan
E-mail: tomek@bci-lab.info (▽corresponding author)
Website: http://bci-lab.info/

***Abstract*—We present a study of a support vector machine (SVM) application to brain–computer interface (BCI) paradigm. Four SVM kernel functions are evaluated in order to maximize classification accuracy of a four classes–based BCI paradigm utilizing a code–modulated visual evoked potential (cVEP) response within the captured EEG signals. Our previously published reports applied only the linear SVM, which already outperformed a more classical technique of a canonical correlation analysis (CCA). In the current study we additionally test and compare classification accuracies of polynomial, radial basis and sigmoid kernels, together with the classical linear (non–kernel–based) SVMs in application to the cVEP BCI.**

I. Introduction

A code–modulated visual evoked potential (cVEP) is a brain ordinary response to a visual stimulus with determined code–modulated sequence [1], [2], [3]. The cVEP is occurring EEG captured on a scalp when a user gazes at a light source which blinks with a designed code–modulated pseudo–random sequence.

The cVEP response gained recently popularity in application to brain computer interfaces (BCIs) [1], [2], [3], which enable a control of a computer or any machine without body muscular activities [4]. The cVEP is easily evoked by a human brain, thus the BCI–based on this paradigm shall potentially result with higher information transfer rate (ITR) [4], which is a measure commonly used to compare interfacing prototypes.

There are several contemporary approaches to classify multi–class cVEP response–based EEG signals. A canonical correlation analysis (CCA) has been extensively tested already [5], which is a method employing a pattern matching approach to calculate multichannel correlation coefficients used next for the attended stimulus pattern identification. In our previous project we also tested the CCA methods [2] to reproduce the previously mentioned results. We could observe that a support vector machine (SVM) [6] method could improve additionally and statistically significant the results of the CCA as tested on the same user group [3].

The SVM is a classification method, which finds a hyperplane located between the classes [6]. It performs usually well as a general classification method, but the classifier performance depends on many parameters, which have to be tuned in order to optimize resulting accuracies. The SVM's kernel function is one of the critical settings and it highly affects classification accuracy. In our previously reported projects [2] only linear SVM without consideration of alternative kernels for a possible classification accuracy boosting. The kernel function allows for a transformation of the EEG cVEP features to a hyperplane space resulting with more simple discriminability. The above mentioned transformation is very critical in case the original feature space cannot result with linear function based discriminability.

In this paper, we report various SVM kernels' study for cVEP classification accuracy improvement in application to visual BCI paradigms. The tested kernels are: linear (non–kernel); polynomial; radial basis (RBF); and sigmoid [7]. We employ a library LibSVM [7], which is an open source SVM project suitable for our comparison study.

In this study, four types of cVEPs are evoked by visual stimulation using the RGB LEDs, which flash in green–blue and white–black color options. Additionally two carrier frequency are tested of 30 Hz (to compare with regular computer screen–based SSVEP experiments) and 40 Hz (to check feasibility of higher frequency–based BCI paradigms). The four combinations of stimuli are tested and reported in this paper. Additionally, to verify an effect of cVEPs' averaging on the final classification accuracy scores, we also test the numbers of averaging steps in a range of $1 \sim 5$. The averaging procedure usually contributes to a removal cVEP's unrelated noise, which is usually captured together with the EEG signals.

From now on the paper is organized as follows. In the next section we present materials and methods of the study. Results follow and finally conclusions are presented together with future research perspectives.

II. Materials and Methods

The experiments reported in this paper were performed in the Life Science Center of TARA, University of Tsukuba, Japan. All the experimental procedure details and the research targets of the developed within the presented project's visual BCI (cVEP–based) paradigm were explained carefully to the nine participating users. All the users agreed voluntarily to participated in the study and they signed informed consents. There were no monetary compensations for the participating users.

The EEG cVEP–based BCI experiments were conducted in accordance with *The World Medical Association Declaration of Helsinki - Ethical Principles for Medical Research Involving Human Subjects*. The experimental procedures were also approved and peer–reviewed by the Ethical Committee of the Faculty of Engineering, Information and Systems at University of Tsukuba, Tsukuba, Japan (experimental permission no. $2013R7$).

The average age of the users was of 26.9 years old (standard deviation of 7.3 years old). A single female and eight male users participated in the study.

A. Experimental Settings

To evoke the cVEP responses, captured in the continuously recorded EEG signals, the visual stimuli were presented to the user as blinking light sources using the red–green–blue (RGB) LEDs. During the cVEP–based BCI EEG experiments the user was seated on a comfortable chair in front of the four LEDs attached to a rectangular frame as depicted in Figure 1. A distance between user's eyes and the LEDs was about $30 \sim 50$ cm. The exact distance setting was chosen by each user for a comfortable view of the all the four LEDs. The experimental room had an ambient light as in an usual office.

In order to remove power line interference from EEG a notch filter was applied in a frequency band of $48 \sim 52$ Hz. Additionally a band–pass filter to remove eye blinks and high frequency muscle–originating noise was applied in a band of $5 \sim 100$ Hz. Details of the EEG experimental set–up are summarized in Table I. To remove any possibility of capturing user's eye blinks, each trial to gaze at a single LED was separated with several seconds long and user–paced pauses.

Fig. 1. A user holding a frame with four LEDs attached to each edge. The user is wearing the EEG cap and g.USBamp amplifier on the left together with a trigger capturing box g.TRIGbox, all by g.tec medical instruments GmbH, Austria, are also presented. The photograph is reproduced with the user's consent.

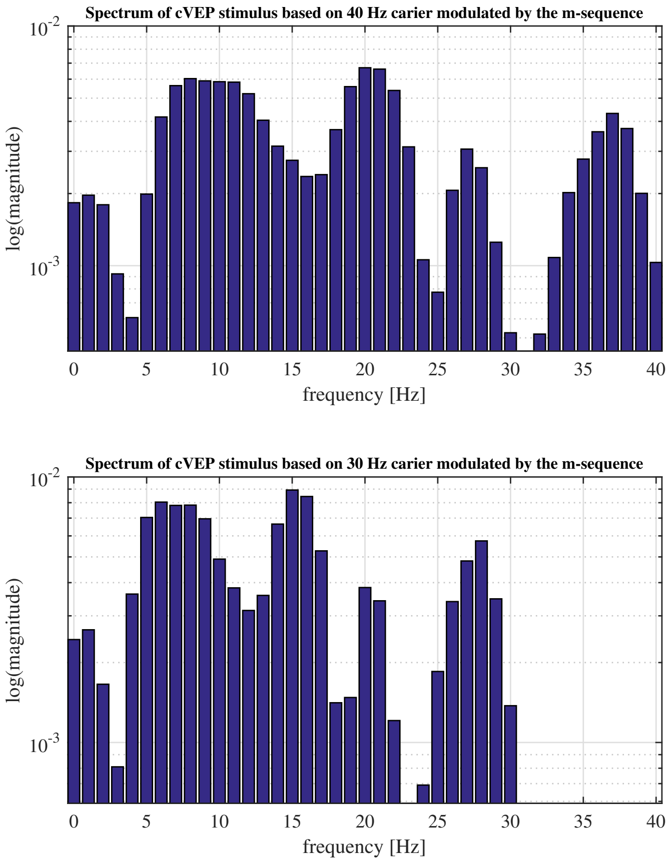

Fig. 2. Spectra of the two visual stimuli generated with the same $m-sequence$ and presented to subjects with two carrier frequencies of 30 Hz and 40 Hz.

The 60 cVEPs were collected for each of four LED blinking with $m - sequences'$ generated targets.

The $m - sequence$ is a binary pseudorandom generated signal, which could be calculated for each latency n as follows,

$$x(n) = x(n-p) \oplus x(n-q), \quad (p > q), \tag{1}$$

where $x(n)$ is the n^{th} element of the $m - sequence$ obtained by the exclusive–or (XOR) operation, denoted by $\oplus$ in the equation (1), using the two preceding elements indicated by their positions $(n-p)$ and $(n-q)$ in the string. In this project $p = 5$ and $q = 2$ were chosen. An initial binary sequence was decided, to create the final $m - sequence$, used in the equation (1), as follows,

$$\mathbf{x}_{initial} = [0, 1, 0, 0, 1]. \tag{2}$$

Finally, the 31 bits long $m-sequence$ was generated based on the above initial string as in equation (2). The spectra of the $m-sequence$ obtained from the equation (1) using initial values listed in (2) have been depicted in Figure 2 clearly supporting a hypothesis of broadband frequency nature of this type of visual stimulus.

The LEDs were controlled from ARDUINO UNO micro–controller board which send square waves reproducing the

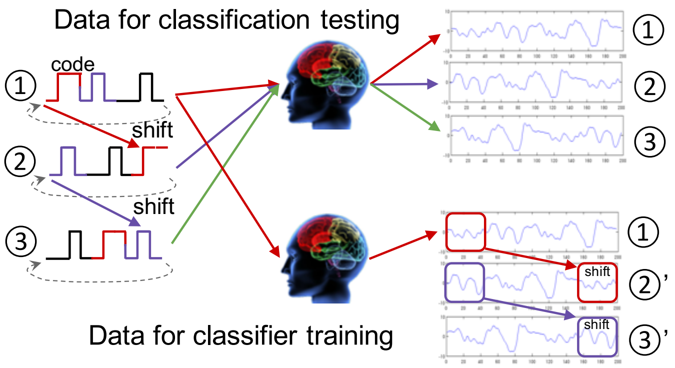

Fig. 3. A procedure of generation cVEP features used in a subsequent SVM classification. The original $m-sequence$ generated by the equation (1) is denoted by ①. In the SVM classifier training session only cVEP features obtained in response to ① were used together with circularly shifted features ②′ and ③′, based on an assumption that the responses ② ≈ ②′ and ③ ≈ ③′. In the cVEP classification accuracy testing session using the above trained SVM the user gazed at each stimulator to evoke separate cVEPs (no more algorithmically shifted).

four $m-sequences$ obtained from circular shifts of the original one. The circular shift on $\tau = 7$ bits was additionally multiplied for the remaining sequences of $2 \cdot \tau$ and $3 \cdot \tau$, respectively. The micro–controlled program was written in C–language by our team.

The $m-sequence$ autocorrelation has a single dominant peak. This feature is beneficial to evoke separable cVEPs (easy to discriminate due to non–periodic patterns by SVM classifiers).

B. The cVEP Responses Classification

Interestingly, only one command dataset is enough for SVM classifier training as shown in Figure 3. The remaining

TABLE I
EEG SIGNALS RECORDING CONDITIONS

Experimental setting	Detail
Number of users	9 (8 males and 1 female)
Average age of users	26.4 years old (standard deviation of 7.0 years)
Single session length	8 or 11 seconds
$m-sequence$ length T	516.7 or 38.75 ms (31 bits)
$m-sequence$ shifts τ	116.7 or 87.5 ms (7 bits)
EEG amplifier	g.USBamp with wet active g.LADYbird electrodes by g.tec medical instruments GmbH Austria
Electrode locations	$O1, O2, Po3, Po4, P1, P2, Oz, Poz$
Reference electrode position	Left earlobe
Ground electrode position	FPz
Sampling frequency	512 Hz
Notch filter	Butterworth 4^{th} order with rejection band of 48 $\sim$ 52 Hz
Band–pass filter	Butterworth 8^{th} order with pass band 5 $\sim$ 100 Hz

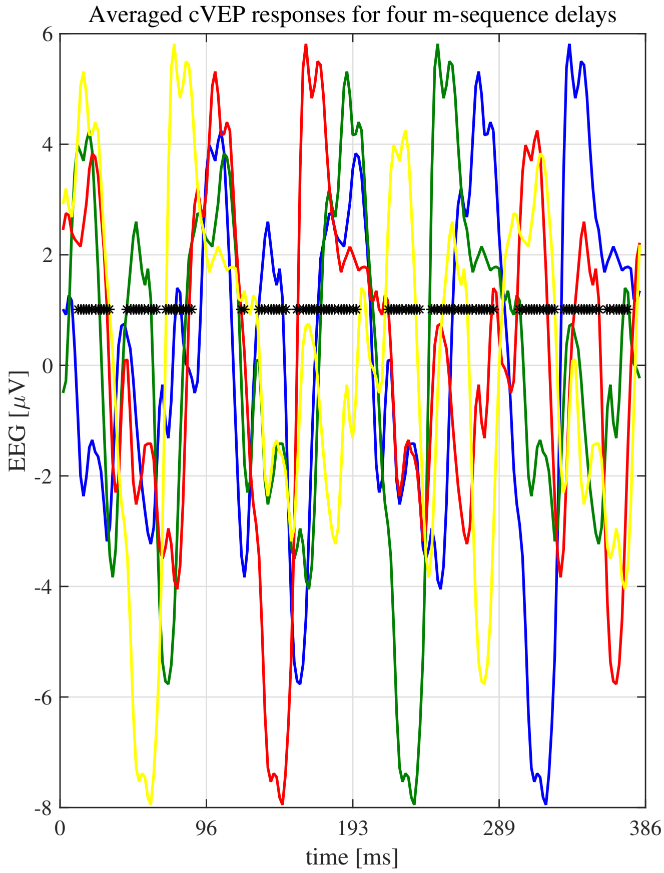

Fig. 4. Averaged cVEP responses with circular shifts. The star symbols ($*$) on a horizontal axis depict the ANOVA estimated statistically significant differences among the latencies ($p < 0.01$) of circularly shifted cVEPs.

classifier training patterns can be generated by circular shift of the cVEP EEG responses similarly as the $m-sequences$ could be obtained using the same process illustrated in Figure 3.

The 60 cVEP responses for only single command #1 (located at the top of the frame presented in Figure 1) were recorded twice in order to use them for classifier's training and testing separately. The remaining 60 cVEP features (responses to the bottom, right and left stimulators as shown also in Figure 1) were captured only once for the classification testing procedure. Totally 300 responses were recorded in the single experimental session.

In the SVM classifiers' training and testing sessions (for all kernels including linear, polynomial, radial basis, and sigmoid), the averaged cVEPs formed a single feature as follows,

$$\bar{\mathbf{y}}_{i,l} = \frac{1}{M} \sum_{j=l}^{l+M-1} \mathbf{y}_{i,j}, \tag{3}$$

where $M = 1, 2 \ldots 5$, and $y_{i,l}$ was the averaged cVEP evoked by the stimulator $i = (1, 2, 3, 4)$. $l = 1, 2, \ldots, N - M + 1$ was the dataset number. In the both SVM classifier training and testing sessions the same number of $M = 1, 2 \ldots 5$ of cVEP averages were used for features' generation.

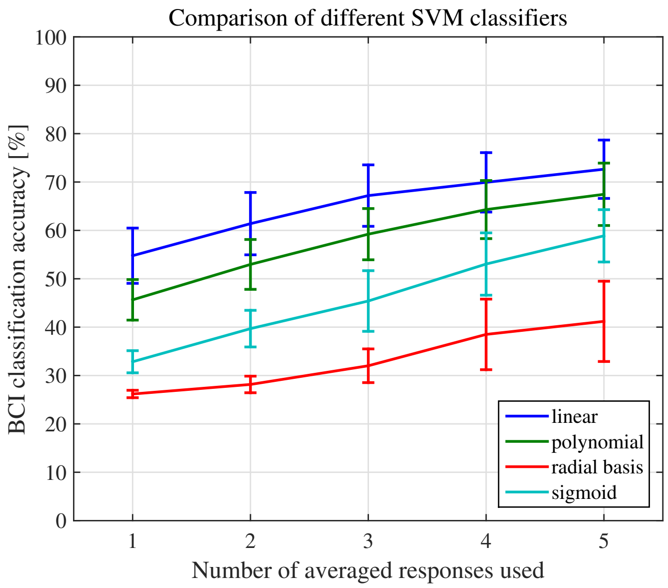

Fig. 5. Classification results of the four SVM kernel function types in application to cVEP responses using green–blue LEDs and carrier frequency of 40 Hz. The mean line scores are surrounded by standard error bars calculated from averaged responses. The horizontal axis represents the number of cVEP averages ($M = 1, 2 \ldots 5$) used to remove EEG noise.

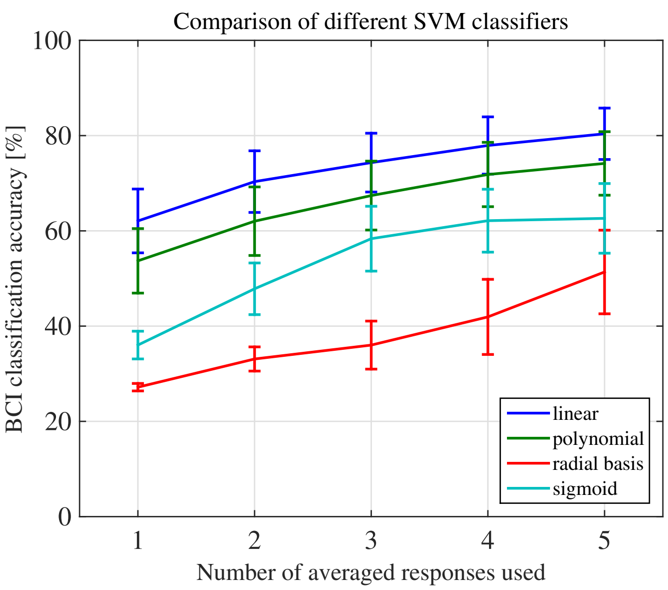

Fig. 6. Classification results of the four SVM kernel function types in application to cVEP responses using green–blue LEDs and carrier frequency of 30 Hz. The mean line scores are surrounded by standard error bars calculated from averaged responses. The horizontal axis represents the number of cVEP averages ($M = 1, 2 \ldots 5$) used to remove EEG noise.

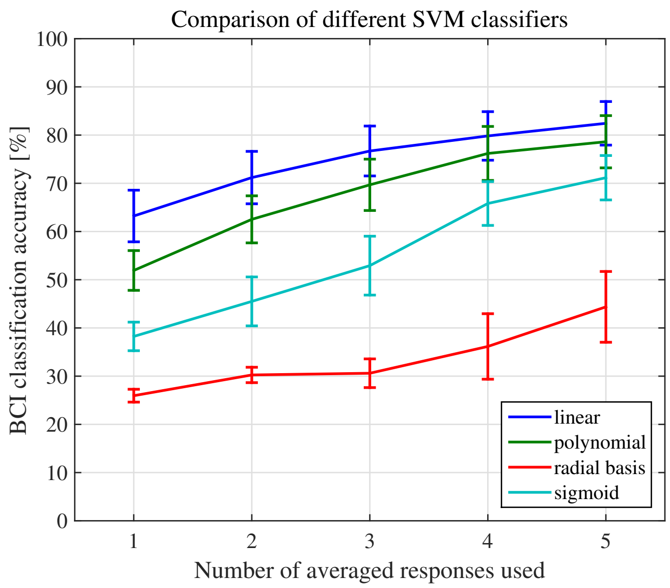

Fig. 7. Classification results of the four SVM kernel function types in application to cVEP responses using white–black LEDs and carrier frequency of 40 Hz. The mean line scores are surrounded by standard error bars calculated from averaged responses. The horizontal axis represents the number of cVEP averages ($M = 1, 2 \ldots 5$) used to remove EEG noise.

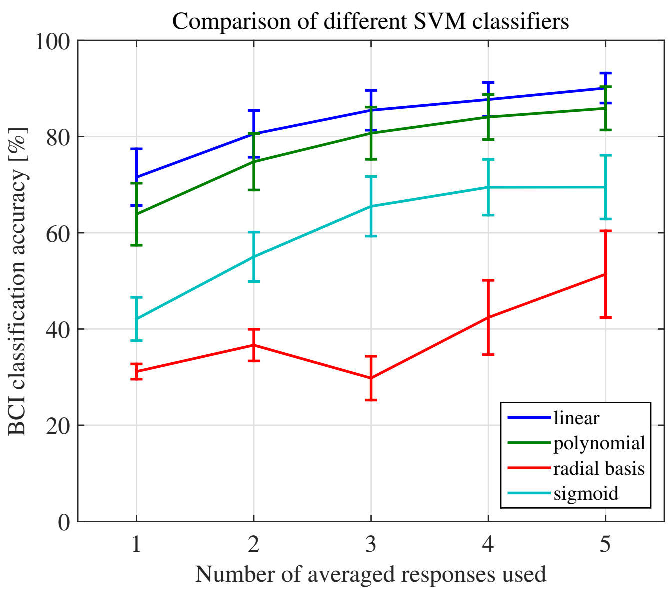

Fig. 8. Classification results of the four SVM kernel function types in application to cVEP responses using white–black LEDs and carrier frequency of 30 Hz. The mean line scores are surrounded by standard error bars calculated from averaged responses. The horizontal axis represents the number of cVEP averages ($M = 1, 2 \ldots 5$) used to remove EEG noise.

III. Results

The classification results of the presented evaluation of four SVM classifiers for cVEP–based BCI prototype have been presented in form of error–bar plots in Figures 5, 6, 7, and 8 and averaged accuracies in Table II.

The results have shown that the linear SVM scored the best for of the all tested cVEP cases (see Figures 5, 6, 7, and 8). The polynomial, sigmoid and radial basis kernels scored with lower accuracies. Especially, the sigmoid kernel SVM classification accuracy with non averaged cVEP (number of cVEPs equal to one in Figures 5, 6, 7, and 8) resulted with theoretical chance level of 25%. The larger the number of averaged cVEPs

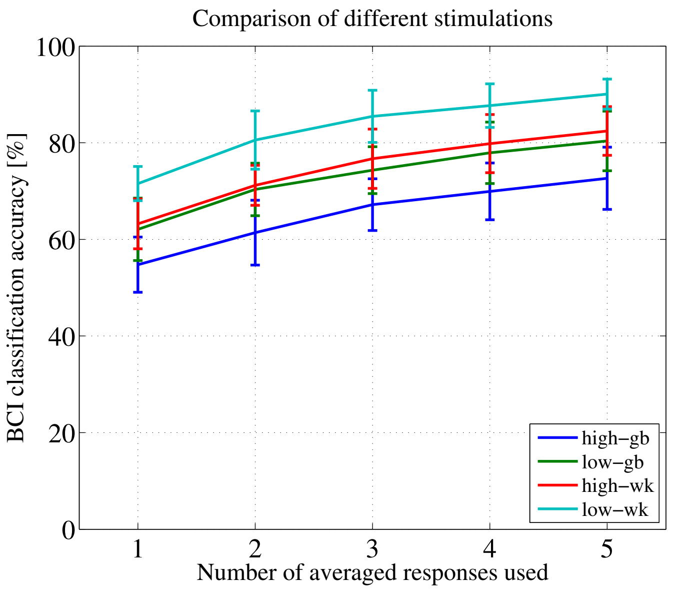

Fig. 9. Classification results of the four stimulation types using linear SVM. The mean line score are surrounded by standard error bars calculated from averaged responses. The horizontal axis represent the number of cVEP averages used to remove EEG remove noise.

were used, the better SVM classification accuracy results were obtained for all the tested kernels as clearly visualized with a positive trend of averaged results in Figures 5, 6, 7, and 8.

The classification results of the linear SVM have been also compared among the stimulation types as depicted in Figure 9 and summarized in Table III. The results have shown that white–black cVEP with 30 Hz carrier frequency scored the best for any number of response averages used.

TABLE II
FIVE ERP AVERAGES–BASED CVEP CLASSIFICATION ACCURACY RESULTS WITH FOUR KERNEL FUNCTIONS AND FOUR VISUAL STIMULATION TYPES

LED light colors and visual stimulation types	SVM kernel type and resulting accuracies			
	linear	polynomial kernel	radial basis kernel	sigmoid kernel
green & blue with 40 Hz carrier frequency	72.64%	67.46%	41.20%	58.88%
green & blue with 30 Hz carrier frequency	82.44%	78.62%	44.37%	71.16%
white & black with 40 Hz carrier frequency	80.38%	74.16%	51.36%	62.62%
white & black with 30 Hz carrier frequency	90.08%	85.86%	51.39%	69.49%

TABLE III
P–VALUES OF MULTI–COMPARISON CALCULATED BY TUKEY–KRAMER METHOD IN CASE OF LINEAR SVM (THE "$*$" SYMBOLS MARK THE RESULTS WITH $p \leq 0.05$)

LED light colors and stimulation types	Multi–comparison Tukey–Kramer calculated p–values using different numbers of averaged cVEP responses				
	No	2	3	4	5
green & blue with 40 Hz carrier versus green & blue with 30 Hz	0.111	0.030*	0.102	0.046*	0.043*
green & blue with 40 Hz carrier versus white & black with 40 Hz	0.047*	0.014*	0.013*	0.007*	0.005*
green & blue with 40 Hz carrier versus white & black with 30 Hz	0.000*	0.000*	0.000*	0.000*	0.000*
green & blue with 30 Hz carrier versus white & black with 40 Hz	0.986	0.994	0.873	0.927	0.898
green & blue with 30 Hz carrier versus white & black with 30 Hz	0.019*	0.009*	0.002*	0.008*	0.006*
white & black with 30 Hz carrier versus white & black with 40 Hz	0.051	0.021*	0.026*	0.052	0.047*

On the other hand, the green–blue cVEP with 40 Hz carrier frequency resulted with lowest accuracies. There were no statistically significant differences of classification accuracies among the white–black cVEPs with 40Hz carrier frequencies and green–blue with 30 Hz, respectively, as summarized in Table III.

IV. CONCLUSIONS

In this paper we have shown a comparison of four SVM kernel function–based classification accuracy results of the cVEP brain responses in application to the visual BCI. As a clear result of the conducted study the linear SVM was identified as the best classifier of cVEP responses in comparison to polynomial, radial basis and sigmoid kernels. Additionally, the BCI classification accuracies in case of the white–black and 30 Hz carrier frequency cVEPs resulted with the best scores in case of linear SVM application.

Also the averaging procedure of cVEP responses clearly enhanced the SVM classification outcomes for all of the tested kernels.

We plan to continue this line of research to develop safe, non–annoying and possibly benefiting the future users of visual BCIs in need.

Acknowledgments

We would like to thank Dr. Andrzej Cichocki from RIKEN BSI, Japan, and Dr. Koichi Mori from Research Institute of National Rehabilitation Center for Persons with Disabilities, Japan, for very stimulating discussions about chromatic SSVEP–based BCI which stimulated this project.

References

[1] G. Bin, X. Gao, Y. Wang, B. Hong, and S. Gao, "VEP-based brain-computer interfaces: time, frequency, and code modulations [Research Frontier]," *Computational Intelligence Magazine, IEEE*, vol. 4, no. 4, pp. 22–26, 2009.

[2] D. Aminaka, S. Makino, and T. M. Rutkowski, "Chromatic and high–frequency cVEP–based BCI paradigm," in *2015 37th Annual International Conference of the IEEE Engineering in Medicine and Biology Society (EMBC)*, IEEE Engineering in Medicine and Biology Society. IEEE Press, August 25–29, 2015, pp. 1906–1909. [Online]. Available: http://arxiv.org/abs/1506.04461

[3] ——, "Classification accuracy improvement of chromatic and high–frequency code–modulated visual evoked potential–based bci," in *Brain Informatics and Health*, ser. Lecture Notes in Computer Science, Y. Guo, K. Friston, F. Aldo, S. Hill, and H. Peng, Eds. Springer International Publishing, 2015, vol. 9250, pp. 232–241. [Online]. Available: http://dx.doi.org/10.1007/978-3-319-23344-4_23

[4] J. Wolpaw and E. W. Wolpaw, Eds., *Brain-Computer Interfaces: Principles and Practice*. Oxford University Press, 2012.

[5] G. Bin, X. Gao, Y. Wang, Y. Li, B. Hong, and S. Gao, "A high-speed BCI based on code modulation VEP," *Journal of Neural Engineering*, vol. 8, no. 2, p. 025015, 2011.

[6] V. Vapnik, *The Nature of Statistical Learnig Theory*. Springer Verlag, 1995.

[7] C.-C. Chang and C.-J. Lin, "LIBSVM: A library for support vector machines," *ACM Transactions on Intelligent Systems and Technology*, vol. 2, pp. 27:1–27:27, 2011, software available at http://www.csie.ntu.edu.tw/~cjlin/libsvm.